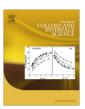
FISFVIFR

Contents lists available at SciVerse ScienceDirect

Journal of Colloid and Interface Science

www.elsevier.com/locate/jcis



23 Na and $^{35/37}$ Cl as NMR probes of growth and shape of sodium taurodeoxycholate micellar aggregates in the presence of NaCl

Fioretta Asaro ^{a,*}, Luigi Feruglio ^a, Luciano Galantini ^b, Alessia Nardelli ^a

ARTICLE INFO

Article history: Received 16 July 2012 Accepted 20 September 2012 Available online 13 October 2012

Keywords: T₁ DQF Quadrupole splitting Bile salts NaCl NaBr Anisometry

ABSTRACT

The growth of the aggregates of the dihydroxylated bile salt sodium taurodeoxycholate (NaTDC) upon NaCl addition and the involvement of the counterion were investigated by NMR spectroscopy of monoatomic ionic species. 23 Na T_1 values from 0.015, 0.100, and 0.200 mol kg $^{-1}$ NaTDC solutions in D $_2$ O, at variable NaCl content, proved to be sensitive to the transition from primary to secondary aggregates, which occurs in the former sample, and to intermicellar interaction. Some 79 Br NMR measurements were performed on a 0.100 mol kg $^{-1}$ NaTDC sample added by NaBr in place of NaCl for comparison purposes. The 23 Na, 35 Cl, and 37 Cl double quantum filtered (DQF) patterns, from the 0.100 mol kg $^{-1}$ NaTDC sample, and 23 Na ones also from the 0.200 mol kg $^{-1}$ NaTDC one, in the presence of 0.750 mol kg $^{-1}$ NaCl, are a clear manifestation of motional anisotropy. Moreover, the DQF spectra of 23 Na and 37 Cl, which possess close quadrupole moments, display a striking similarity. The DQF lineshapes were simulated exploiting the Scilab environment to obtain an estimate of the residual quadrupole splitting magnitude. These results support the description of NaTDC micelles as cylindrical aggregates, strongly interacting at high ionic strengths, and capable of association with added electrolytes.

© 2012 Elsevier Inc. All rights reserved.

1. Introduction

Bile salts are a class of anionic amphiphiles of natural origin characterized by a rigid steroidal nucleus, which bears a few OH groups and a short lateral chain ending with a charged head-group. The convex side of the condensed ring system, termed β , with two methyl groups, corresponds to the polar moiety. The sickle shape endows the molecules with three axial chirality [1].

They are involved in many physiologically and pathologically relevant processes [2–6] in vivo and the biomedical significance drove the intense research of the early times, the second half of last century. At present, the interest toward such compounds is not fading, stimulated by the increasing technological relevance and their use [7–13], also as semisynthetic derivatives [14–17], in the materials of future.

The peculiar self-aggregation behavior of these molecules, which remarkably differs from that of common surfactants, plays a paramount role in the practical application. It is phenomenologically well characterized, owing to the many investigations, carried out by a broad array of techniques. The correspondingly copious literature has been summarized in various reviews [2,18], also recently [19,20]. In spite of this, the supramolecular arrangement

E-mail addresses: fasaro@units.it (F. Asaro), luigi.feruglio@yahoo.it (L. Feruglio), l.galantini@caspur.it (L. Galantini), giallotweety@libero.it (A. Nardelli).

in bile salts micelles remains not fully understood. It is described by means of various widely different models, which imply correspondingly different morphologies. The most popular, and commonly used, ones [20] range from the first model, proposed by Small, of elongated secondary micelles [21] to those of disklike aggregates [22] and of elongated helical geometry [23]. Theoretical methods, as well, were invoked in order to get insight into the subtle interplay of polar and hydrophobic interactions and hydrogen bonds, certainly quite different than in micelles of classical surfactants, ruling the micellar structure. The molecular dynamics calculation outcomes are in line with the Small model and suggest an irregular morphology [24]. However, owing to the high complexity and delicacy of the matter, the comparison with reliable experimental results of micellar morphology is mandatory. Here, we aim at providing experimental information on the morphology of bile salts assemblies, in particular at high ionic strength, at which the aggregates are rather large, from a new, unexplored point of view, namely the one of the sodium counterion and of the co-ions of the added electrolyte, in order to improve the structural modellization of these peculiar self-assemblies.

Indeed, NMR spectroscopy of the nuclei of sodium and of halides, conventional counterions, has frequently been employed in the study of structure and dynamics of micellar and biopolyelectrolytes systems [25–27]. Besides relaxation times, we have employed double quantum filtered (DQF) experiments, suited to soft

^a Department of Chemical and Pharmaceutical Sciences, University of Trieste, via L. Giorgieri 1, 34127 Trieste, Italy

^b Department of Chemistry, University of Rome "La Sapienza", P. le A. Moro 5, 00185 Rome, Italy

^{*} Corresponding author. Fax: +39 0405583903.

matter [28–32], because they are capable of enlightening in a straightforward manner, just through the spectral pattern, slow motions' contributions to relaxation [33,34] and, even unresolved, quadrupolar splitting [28]. The latter is a distinctive feature of slight motional anisotropy in incompletely disordered systems.

Sodium taurodeoxycholate (NaTDC), considered in the present study, belongs to the class of dihydroxylated bile salts, well known to give rise to aggregates that grow to a great extent upon increasing both concentration and medium's ionic strength [35–37].

2. Experimental section

2.1. Preparation of samples

NaTDC purchased by Sigma was crystallized twice from a mixture of water and acetone. D_2O 99.9% (CIL) was employed as solvent.

Three solutions, at different NaTDC concentration, namely 0.015, 0.100 and 0.200 mol kg $^{-1}$, were prepared by weight. The NaCl concentration was increased by adding the appropriate amounts of solid NaCl. A 0.100 mol kg $^{-1}$ NaTDC solution was studied also in the presence of NaBr instead of NaCl.

2.2. NMR measurements

The NMR measurements were performed, at 303 K, on a JEOL Eclipse 400 spectrometer (9.4 T) operating at 400 MHz for $^{1}\mathrm{H}$ and 105.75 MHz for $^{23}\mathrm{Na}$, 39.17 MHz for $^{35}\mathrm{Cl}$, 32.60 MHz for $^{37}\mathrm{Cl}$ and 100.16 MHz for $^{79}\mathrm{Br}$, equipped with a JEOL NM-EVTS3 variable temperature unit.

The 23 Na longitudinal relaxation times, T_1 , were determined by inversion recovery using 19 intervals, accumulating 64 transients for each interval, employing a spectral width of 600 Hz over 1 K complex data points.

The ⁷⁹Br transverse relaxation rates ($R_2 = 1/T_2$) were determined from the line-width at half-height ($\Delta v_{1/2}$) of the signals present in the spectra, acquired using a spectral width of 30 kHz over 8192 complex data points, from the very same solution used for the ²³Na R_1 measurements, by the relation $R_2 = \pi \Delta v_{1/2}$, since the magnetic field inhomogeneity contribution to line-width is negligible for ⁷⁹Br.

The 23 Na double quantum filtered (DQF) spectra were performed on two samples, containing NaTDC at 0.100 and 0.200 mol kg $^{-1}$ concentration, respectively, and 0.750 mol kg $^{-1}$ NaCl, using the pulse sequence reported in the literature [34] employing two $\pi/2$ pulses for the filter. 288 transients for each τ interval were accumulated, and the τ values for the former sample were 3.2,6,20, and 60 ms along with a spectral width of 600 Hz over 1 K complex data points, while for the latter, they were 1.6,3.2 and 6 ms, and the spectral width 2644 Hz over 8 K data points.

For chlorine nuclei, the DQF experiment was carried out on the former sample employing a spectral width of 600 Hz and 1 K complex data points, with 128 scans and τ values of 2,2.9,4.2, and 10.8 ms for 35 Cl and with 256 scans and τ values of 3,5,7, and 19 ms for 37 Cl.

The DQF can be briefly and efficaciously described, making reference to the expansion of the density operator in terms of irreducible tensor operators [33,34,38,39] and to the Redfield theory of relaxation [40]. Accordingly, the initial $\pi/2$ pulse converts the equilibrium longitudinal magnetization into single quantum coherences (SQCs) of the first rank. During the following τ interval, they evolve partially without changing rank, according to either f_{11} or f_{11} coefficient [39], and partially are converted into SQCs of higher rank. SQC of the third rank may be originated for 3/2 spin quantum

number nuclei, like those here considered, by both biexponential transverse relaxation and residual quadrupolar splitting, f_{31} or f_{31} [39], while SQCs of the second rank are exclusively due to the presence of residual quadrupolar splitting, f_{21} or f_{21} [39]. The analytical forms of the relevant coefficients depend on the relative magnitude of the residual quadrupolar splitting, ω_0 , and of the spectral density at twice the Larmor frequency, J($2\omega_0$), namely [39]:

If $J(2\omega_0) < \omega_0$

$$F_{11}(t) = \frac{3}{5} \left[\cos(\omega_{eff} t) + \frac{J(2\omega_0)}{\omega_{eff}} \sin(\omega_{eff} t) \right] \exp(-R_{2f} t) + \frac{2}{5}$$

$$\times \exp(-R_{2s} t)$$
(1)

$$f_{21}(t) = f_{12}(t) = i\sqrt{\frac{3}{5}} \frac{\omega_{\rm Q}}{\omega_{\rm eff}} \sin(\omega_{\rm eff} t) \exp(-R_{2f} t)$$
 (2)

$$\begin{split} f_{31}(t) &= f_{13}(t) \\ &= \frac{\sqrt{6}}{5} \left[\cos(\omega_{eff} t) + \frac{J(2\omega_0)}{\omega_{eff}} \sin(\omega_{eff} t) \right] \exp(-R_{2f} t) \\ &- \frac{\sqrt{6}}{5} \exp(-R_{2s} t) \end{split} \tag{3}$$

where $\omega_{eff} = \sqrt{\omega_{\rm Q}^2 - J(2\omega_0)^2}$ On the contrary, if $J(2\omega_0) > \omega_{\rm Q}$

$$\begin{split} f_{11}'(t) &= \frac{3}{5} \left[\cosh(\mu_{eff} \ t) + \frac{J(2\omega_0)}{\mu_{eff}} \sinh(\mu_{eff} \ t) \right] \exp(-R_{2f} \ t) + \frac{2}{5} \\ &\times \exp(-R_{2s} \ t) \end{split} \tag{4}$$

$$f_{21}'(t) = f_{12}'(t) = -i\sqrt{\frac{3}{5}} \frac{\omega_{Q}}{\mu_{eff}} \sinh(\mu_{eff} t) \exp(-R_{2f} t)$$
 (5)

$$\begin{split} f_{31}'(t) &= f_{13}'(t) \\ &= \frac{\sqrt{6}}{5} \left[\cosh(\mu_{eff} \ t) + \frac{J(2\omega_0)}{\mu_{eff}} \sinh(\mu_{eff} \ t) \right] \exp(-R_{2f} \ t) \\ &- \frac{\sqrt{6}}{5} \exp(-R_{2s} \ t) \end{split} \tag{6}$$

with $\mu_{e\!f\!f}=\sqrt{J(2\omega_0)^2-\omega_0^2}$ The two transverse relaxation rates, R_2 , denoted by the subscripts f and s, suggestive of fast and slow, can be expressed by the values taken at various frequencies, namely $0,\omega_0$ and $2\omega_0$, of the spectral density function, J, of the motional processes involved in relaxation.

$$R_{2f} = J(0) + J(\omega_0) + J(2\omega_0) \tag{7}$$

$$R_{2s} = J(\omega_0) + J(2\omega_0) \tag{8}$$

The π pulse at the middle of τ interval refocuses chemical shift effects. At the end of τ , the double quantum filter (DQF), made of two pulses coupled with the opportune phase cycle, blocks the SQCs of the first rank letting through those of second and third ranks. During the following acquisition period, the higher rank SQCs evolve back into first rank ones, the very NMR observable, according to coefficients f_{21} and f_{31} . The eventual signal in the frequency domain is the Fourier transform of the sum of f_{12} and f_{13} in time domain, weighed by the factors acquired due to evolution during the τ interval.

2.3. Fitting of DQF spectra

The DQF spectral patterns were calculated according to Eqs. (2), (3) and (5), (6), Fourier Transformed to the frequency domain and weighted by intensity factors due to evolution during τ , which

Download English Version:

https://daneshyari.com/en/article/7000493

Download Persian Version:

https://daneshyari.com/article/7000493

Daneshyari.com